VORTEX STRUCTURES IN THE WAKE OF INCLINED CYLINDERS

Kapil Varshney
Taitem Engineering, PC, Ithaca, NY, 14850, USA

ABSTRACT

In this experimental study, vortex structures in the wake of inclined slender cylinders' tip have been investigated. Thin cylinders of various diameters between 0.5 *mm* to 3.5 *mm* with large aspect ratios (>> 1) have been exposed to low Reynolds number (*Re*) flow starting from *Re* = 150 to 2000. The cylinders were mounted at an angle of attack "α" which was varied from 30^0 to 90^0. Vortex shedding frequencies in conjunction with associated Strouhal numbers of the vortices behind the inclined cylinder have been studied which increased from 0.9 to 1.15 as the angle of attack was decreased from 60^0 to 30^0, and remained nearly constant to the change of Reynolds number. It was also found that these vortices were very stable at low *Re*<700 and vanished quickly at high *Re*>1000. In addition, the stability of these vortices is also dependent on the angle of attack. It was found that these vortices were very sharp and stable at $\alpha = 45^0$ and started becoming unstable as the angle of attack increased or decreased from 45^0.

Keywords: *Flow visualization, Vortex shedding, Laminar flow, Inclined cylinders.*

1. INTRODUCTION

Wake of a rigid body has been one of the most important topics in fluid dynamics for over a century due to its significance in various industrial applications such as vortex shedding behind airplane wings, behind wind turbines, behind low and high rise buildings, chimneys etc. Therefore, in-depth studies on the characteristics of the wakes behind these solid structures have been performed [1–12]. In particular, a circular cylinder wake has been investigated in many previous studies. The wake of circular cylinders in cross flow is widely known as a von K*arma*n vortex street which is composed of equally spaced vortices of the same strength but alternating in sign and they grow in size as they convected downstream. This characteristic (periodicity) of the vortex shedding has been exploited in a vortex counter as mass-flux meter and vortex gas flow-meter, and more recently, an energy harvester for drawing energy from K*arma*n vortex street behind a bluff body in water has been developed which converts flow energy produced by the oscillations of a piezoelectric film into electrical energy [13]. However on the other hand, due to the drag and periodicity of these vortices make them undesirable in few cases such as at the time of landing of an airplane, noise generates due to the vortices shedding behind a wing in a high-lift configuration, and aero-elastic resonances between wakes and elasticity modes of high-rise buildings, chimneys, and bridges could be hazardous.

Vortex dynamics of circular cylinder wake has been thoroughly presented by Williamson [14]. Zdrakovich [15, 16] summarized most of the well known findings related to the flow past a circular cylinder. The wake of a cylinder has been studied for a wide range of *Re*. In an earlier study, boundary layer distributed by a circular cylinder for various gap ratios was presented [17]. It was shown that in the inner region, boundary layer recover faster than in the outer region. Vortex structure and pressure distribution along a circular cylinder mounted in a boundary layer was measured by Bearman & Zdravkovich [18] and they showed that vortex shedding is restricted for gap ratios less than the critical gap ratio of 0.3. The wake structure of a cylinder is a function of the driving frequency of the cylinder. A dimensionless parameter, the Strouhal number ($St = fd/U$), is used to characterize the frequency of these vortex shedding which, based on previous studies, for a cylinder is approximately 0.21 for any Reynolds number greater then 400. The vortex-splitting in the wake of circular cylinders and the emergence of a secondary vortex street in the far wake which evolve due to the formation of pairs of vortices with oppositely-signed strength has been observed by Karasudani & Funakoshi [19]. Wu *et al.* [20] found longitudinal vortices between the Karman vortices in the wake of circular cylinders at low *Re* which have levels of vorticity almost double than that of the Karman vortices while the levels of circulation are typically an order of magnitude less (approximately 11%). Carmo *et al.* [21] modeled the evolution of a three-dimensional mode as a dynamical oscillator using the Landau equation for staggered circular cylinders for studying the wake transitions. Mandal & Dey [22] investigated wake-induced boundary layer transition using the PIV (Particle Image Velocimetry) technique in the wake of a circular cylinder. Nicolle & Eames [23] performed an interesting study in which they numerically studied the influence of void fraction on two-dimensional flows past circular arrays of cylinders. In this study, three different void fraction regimes (low, moderate, and high) were investigated at a characteristic *Re* = 2100 and it was shown that at low void

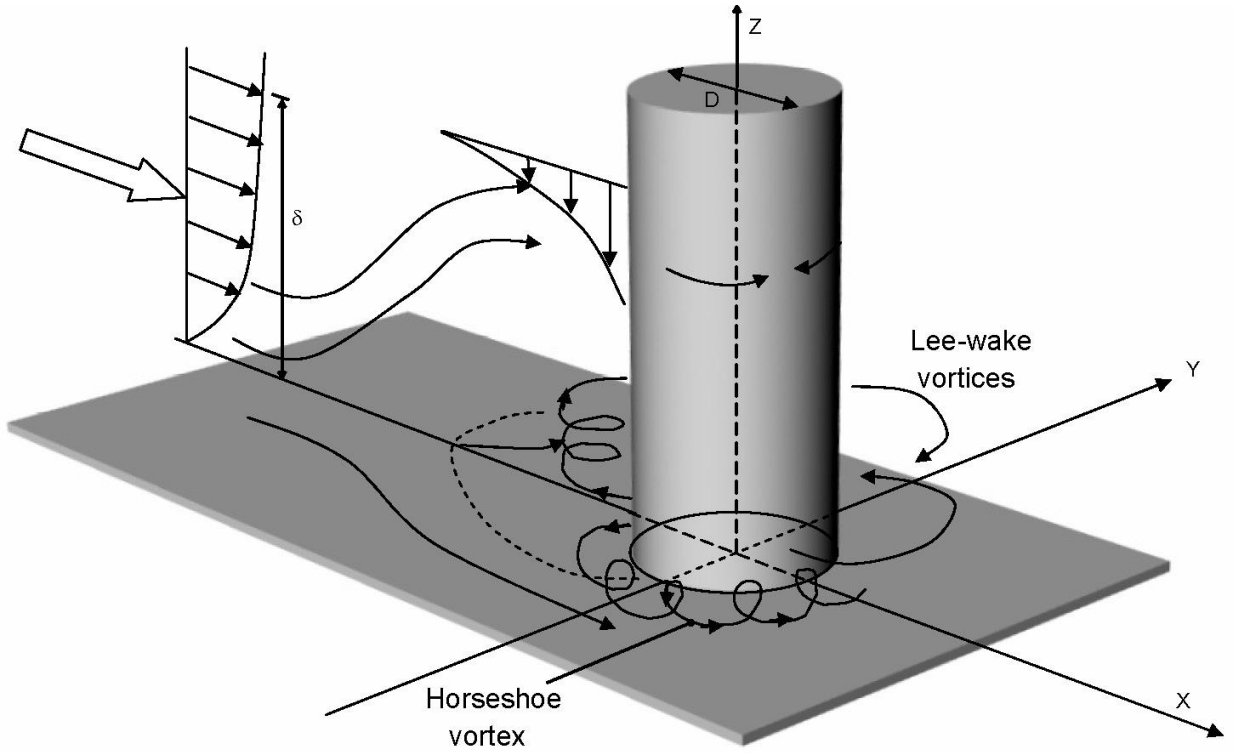

Fig. 1 Definition sketch for flow past vertical cylinder.

fraction regime, the cylinders have uncoupled individual wake patterns, at intermediate void fraction regime, a stable wake form behind the array, and at high void fraction regime, the array produce a wake in a similar fashion to solid body of the same scale.

In an early work on the cylinder wake, laminar and turbulent wakes behind cylinders of different cross sections have been experimentally investigated by Roshko [2] in which he stated that there are some geometric similarities among all vortex streets. In addition, he presented several characteristics of vortex streets that are independent of *Re*, and proposed a general Strouhal number based on the width of the wake. There are other phenomena such as Kelvin Helmholtz instability, boundary-layer e1ects at the obstacle, and transition modes which influence slightly the laminar and turbulent vortex-shedding process without strongly affecting the main characteristics of the vortex street [3, 14, 24, and 25].

Besides circular cylinders, flow characteristics around other shapes such as flat plate, airfoil, airfoil-shaped bluff bodies (i.e. elliptical cylinders), square cylinders, and hexagonal cylinders have also been explored due to their large engineering applications. Flow behavior behind rectangular cylinders has attracted researchers since the experimental work performed by Okajima [26] and later Norberg [27]. Characteristics of elliptical cyliner wake have been explored by Choi & Lee [28] who showed that vortex-shedding frequency decreases with decrease in the gap ratio. Flow structure behind an oscillating NACA 0015 was studied by Birch & Lee [4] at $Re = 1.86 \times 10^5$ and it was shown that the vortex was less organized during pitch-down than during pitch-up. This particular area, the flow around airplane wing, have received significant attention primarily because at the time of landing on the terminals, available altitude may not be available to cope with the problem of rolling or pitching motions induced by the vortices. The vortex structure in the wake of a NACA0012 airfoil with blunt tip was investigated by Devenport *et al.* [29]. A detailed analysis was performed to show the flow structure in the core region and it was also shown that outside the core, the flow structure was dominated by the remainder of the wing wake which wound into an ever-increasing spiral. There are many other prominent experimental and numerical studies in the past which focus on the roll up process of wing-tip vortices, addressing the issues of vortex development, stability, and dynamics of the initial roll-up [4, 30–33]. Sheard *et al.* [34] used an inclined square cylinder and performed numerical simulations on the wake behind it at various incidence angles to expound the three-dimensional stability at low *Re*. In this study, the square cylinder was placed horizontally across the flow and the incidence angle was changed with respect to the incoming flow. Similar study with a square cylinder was performed by Yoon *et al.* [35] in which Floquet stability

analysis was performed to detect the onset of the secondary instability leading to three-dimensional flow. The flow past a square cylinder separates from trailing edge at about *Re* = 50 but remains steady [36] however, above this *Re* it passes through Hopf bifurcation and exhibit periodic oscillatory wake. Further enhancing the *Re* (between 150-200), it becomes three-dimensional but remains time periodic [37].

Accurate and rapid responses from transducers are essential to determine various fluid properties [38–41]. In the cases when fluid is still and an object is freely-falling, high-speed cameras are being used to determine the 3-D orientation and the object speed [42]. In addition to this, there are many other experimental techniques such as Laser-Doppler anemometry (LDA), PIV etc., are being used to measure fluid properties. Roulund *et al.* [43] numerically and experimentally presented the flow around a circular pile. LDA was used in the experiments and the results were used to test, and validate the model. In this study, the flow model was used to investigate the horseshoe vortex and Lee-wake vortex around the vertical cylinder. It was shown that due to the adverse pressure gradient induced by the pile, the upstream boundary layer on the plate leads in a three-dimensional separation and the horseshoe vortex is formed due to the rotation in the incoming flow. A definition sketch for these vortices is shown in Fig. 1. In their previous study, Sumer *et al.* [44] presented that the role of *Re* is reversed because the size of the horseshoe vortex decreased with increasing *Re*. More recently, Shelley & Zhang [45] provided an expository review on the mutual coupling of fluids and flexible bodies which comprises notable experiments and simulation methods that reveal the flow pattern behind flapping and flexible structures. Besides circular and square cylinders, the wake of hexagonal cylinder has also been investigated. Khaledi & Andersson [46] investigated the wake of a hexagonal cylinder numerically for three different *Re* and two different cylinder orientations, and observed higher Strouhal number when *Re* was increased from 100 to 500 however it did not change if *Re* increased further up to 1000.

As stated above, a rich literature is available which comprise in-depth experimental as well as numerical studies on the flow behind circular cylinders. However, the wake of inclined cylinder's tip at various angle of attacks have not been reported previously which is the main motivation of this study. In this article, wake of the inclined cylinders have been explored using dye flow visualization technique and the wake structure is presented at various *Re* and angle of attacks.

2. EXPERIMENTAL SET-UP

In this study, the experiments were carried out in a recirculating, horizontal axis, and closed water tank. The dimensions of the test-section were 46 cm x 15 cm x 15 cm (Fig. 2). During the setting up of the experiment and the initial tests, emphasis was placed on generating actual flow at various *Re*, avoiding any influence on the flow caused by vibrations or other sources. The cylinders were made of stainless steel and plastic. The tips of the cylinders were sanded with fine grit sandpaper to a finish that was smooth to the touch. The smooth tips were required to the low *Re* of the experiments, which negated surface roughness effects. The characteristics of the cylinders used in this study have been summarized in Table 1.

Table 1 Measured and predicted length scale factors using various configurations of passive devices at 40 cm height from the ground level of the wind tunnel

No.	Needle Type	Length (mm)	I.D. (mm)	O.D. (mm)	*Re*
1	Long, Stainless Steel	101.6	1.35	1.65	100 - 3000
2	Short and Thin, Stainless Steel	50.8	0.48	0.71	100 - 3000
3	Short and Thick, Stainless Steel	50.8	1.52	1.83	100 - 3000
4	Long and Thin, Plastic	127.0	2.10	2.30	100 - 3000
5	Long and Thick, Plastic	127.0	3.30	3.50	100 - 3000

Where

I.D. = Inner Diameter
O.D. = Outer Diameter

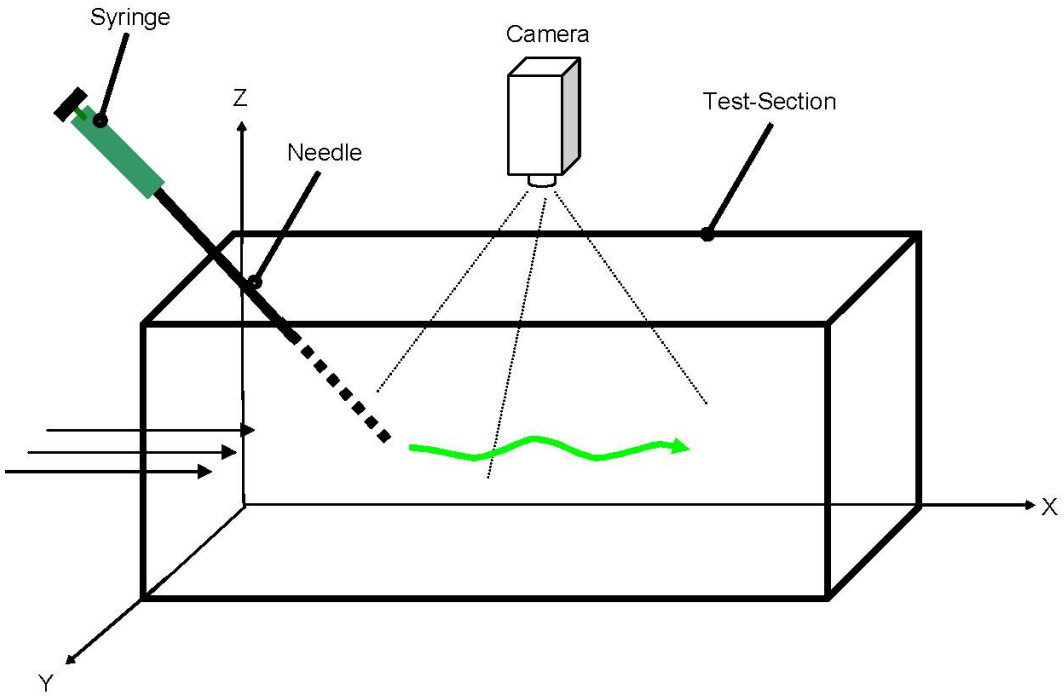

Fig. 2 Schematic view of the experimental recirculating water-tank facility used in this study. Note that the diagram is not to scale.

Under the investigation in this paper, hollow circular cylinders of various diameters in conjunction with syringes, inclined at an angle of incidence (a) to an oncoming free stream with velocity *U* were used. The inner and the outer diameters of the cylinders (Table 1) were measured by digital caliper. A schematic representation of the set-up of the experimental apparatus is shown in Fig. 2. The main test section was equipped with a two-axis mechanical traversing system. The traversing system had an adjustable syringe holder mounted at the end of the moving arm allowing the syringes to be mounted on the traverse at the center of the test section with their tips approximately 5 *cm* into the water. In all reported cases, the angle of attack of the cylinders was varied from 30^0 to 60^0 and the water speed *U1* was varied from 0.65 mm/s to 15 mm/s, which corresponds to Reynolds numbers from 100 to 2000. A Reynolds number and a Strouhal number (*St*) which characterize wake shedding frequencies are defined as,

$$\mathrm{Re} = \frac{UW}{\nu},\ St = \frac{fd}{U} \qquad (1)$$

where ν is the kinematic viscosity of the fluid, *W* is the width of the test section, *d* is the diameter of the cylinder, and *f* is wake shedding frequencies. There have been several techniques adopted by the researchers to visualize vortices in the wake to cylinders. The technique of wake visualization by coating a body in a fluorescent dye was first introduced in the studies of the wake behind a circular cylinder by Williamson [3, 14]. The experimental method employed in the present study differed somewhat from previous experimental studies because prior investigations were mainly focused on the wake of horizontally and vertically mounted cylinders. Because of the desire to capture the wakes behind the inclined cylinders, syringes were filled with Fluorescein dye (Fluorescein sodium salt, F6377) and the dye was slowly injected into the water at a desired angle of attack and *Re*. The dye got trapped in the shape of vortices as they convected downstream.

3. RESULTS AND DISCUSSION

In previous investigations, the flow around the free end of the cylinder has been studied by several authors [47–51]. However, in these studies, vertical cylinders were mounted on a flat plane and the incoming flow was perpendicular to the cylinders. The flow around an inclined cylinder can be complex, showing vortex structures and mechanisms with different properties and different behaviors. The dye flow visualization with homogeneous illumination of the field of view is capable of characterizing the spatial flow structure on a certain position and also reveals the flow pattern of the inclined cylinder wake. The first parameter set of the present investigation was Re ~ 100 and $\alpha = 45^0$. Flow resulting for this parameter combination was stable and very weak disturbances in the cylinder wake were

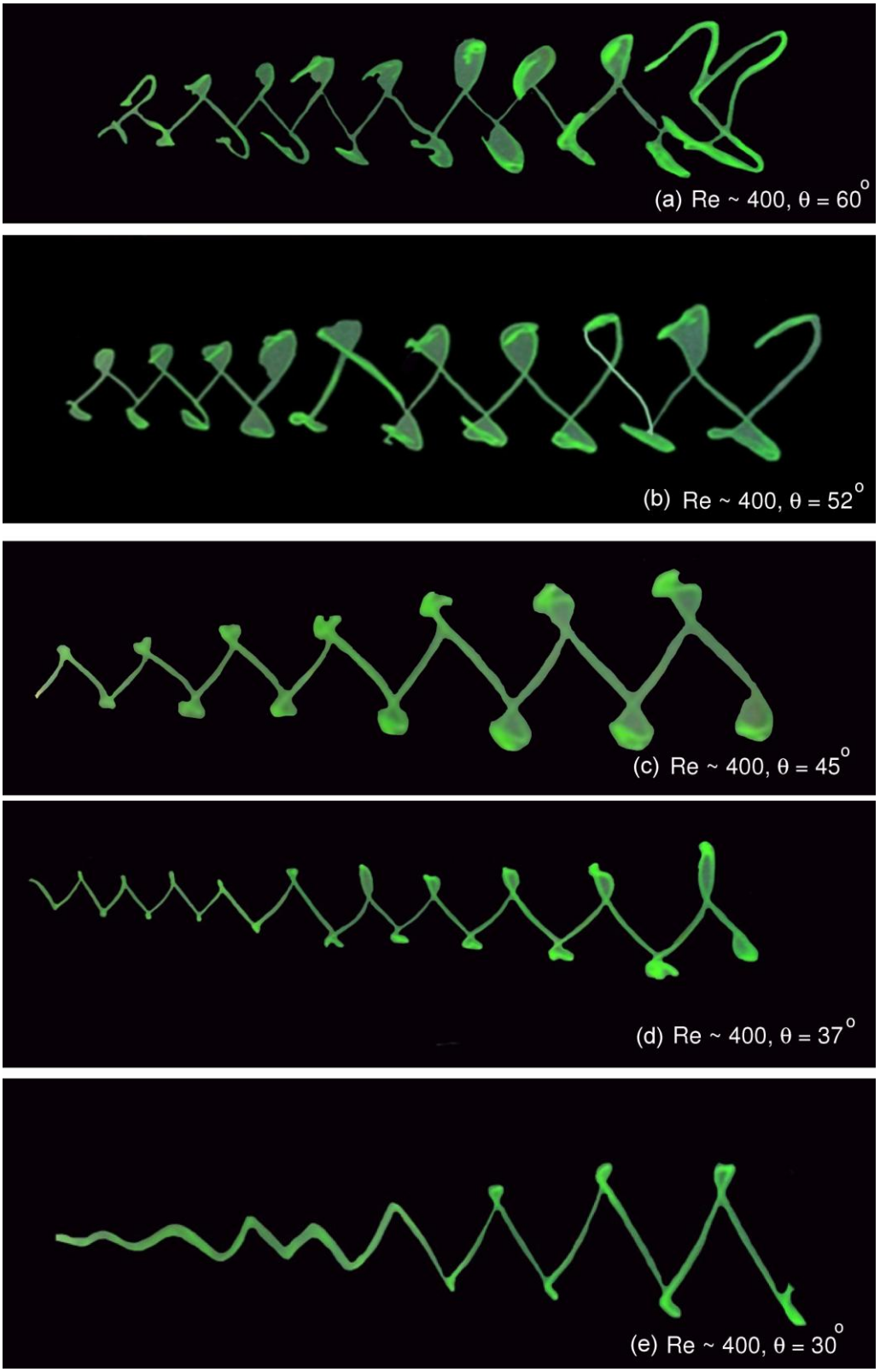

Fig. 3 Top view. Variation in the shape of the vortices as a function of angle of attack. These vortices were generated using the long, stainless steel needle (Table 1) and look more stable and robust at $\alpha = 45^0$observed. Detailed studies by means of flow visualization showed that the resulting flow was three-dimensional and providing stable vortex shedding below *Re* = 700.

Although the dye flow visualization gives various information of the flow pattern in the wake of the inclined cylinders, it is difficult to imagine the spatial configuration far away from the cylinders. In Fig. 3, 4 and 5, a collection of dye flow visualization results are presented with the test-section of the water tank illuminated homogeneously from upstream to downstream. It needs to be pointed out that, due to the fact that the vortex street is generated from the tip of the inclined cylinders, the dye which emanated out from the tip of the inclined cylinders sucked in by the vortex visualized the vortex. All other vortices which are shedding from the other submerged parts of the inclined cylinders took a different route and are not visible in the figures. It should be noted that despite counter rotating feature, these vortices are significantly different from Karman vortices in terms of shape, evolution, and their movement with the flow. Therefore, the vortex street behind the inclined cylinders' tip will be mentioned K-type vortex street hereafter in this article.

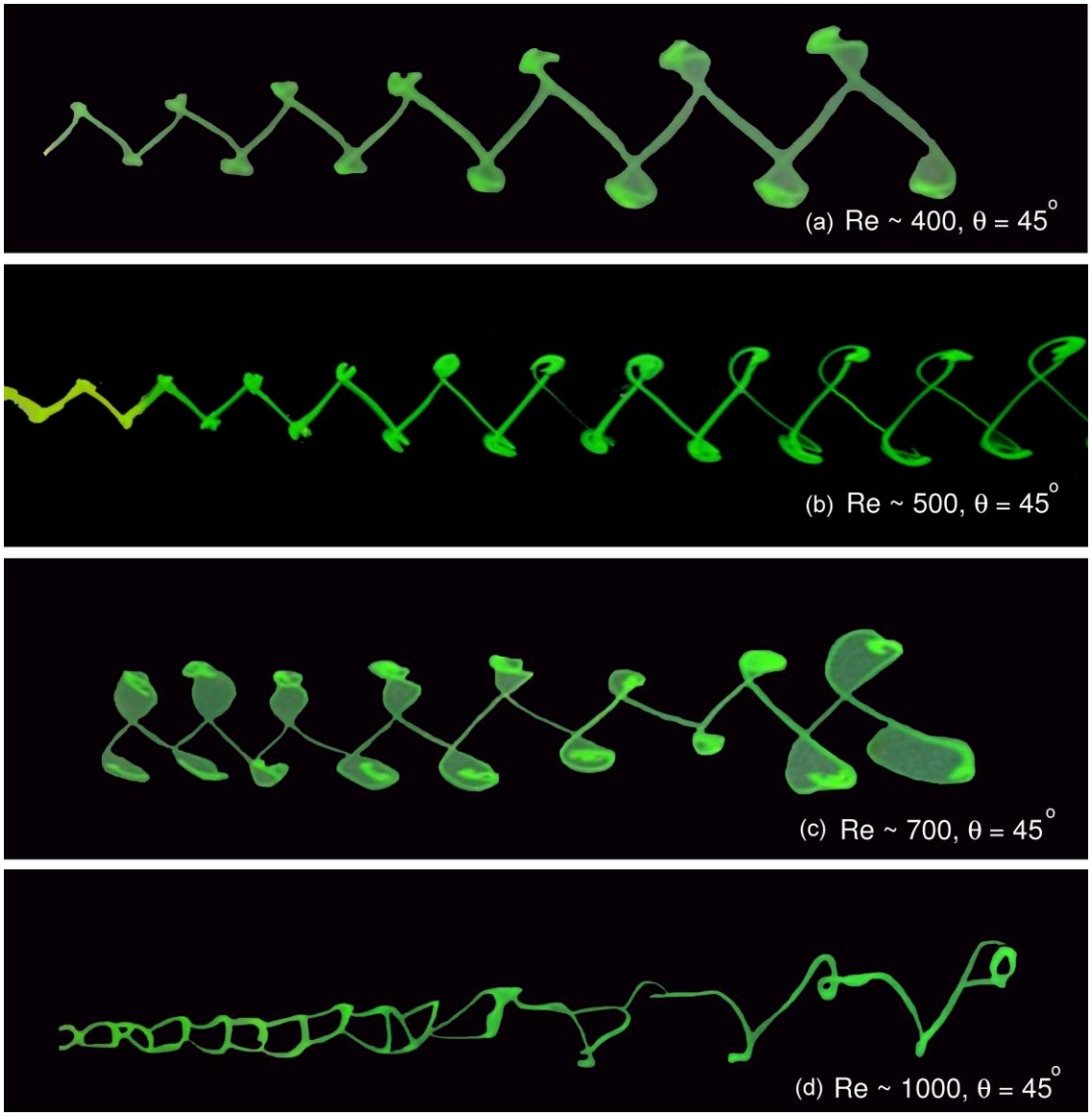

Fig. 4 Top view. Alteration in the shape of vortices as a function of *Re* and fixed angle of attack. Three different states could be distinguished: the development of non-axisymmetric periodic vortex shedding (*Re* < 700), transition from periodic vortex shedding to chaotic motion which comprises distorted vortices (700 > *Re* > 1000), and a state in which the vortices disappear because of *Re* (*Re* > 1000).

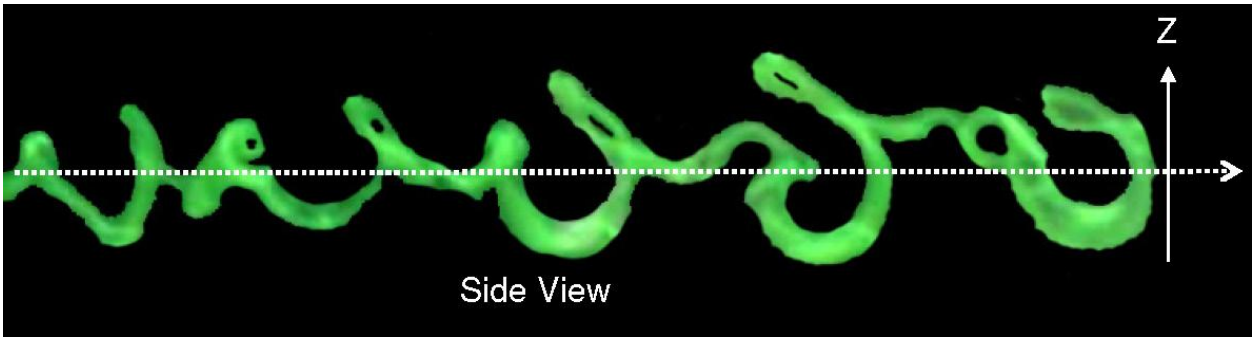

Fig. 5 Side view of the K-type vortices using the big plastic needle (Table 1). In this experiment, *Re* was set at 700 and the angle of attack was 45^0.

Figure 3 shows some typical results of the dye flow visualization under five different angles of attack and at a constant *Re* ~ 400. It can be noted in the figure that the shape of the vortex street depends on α. For a given *Re*, the vortex street looks most stable at $\alpha = 45^0$ (Fig. 3). When the cylinder was mounted perpendicular to the flow ($\alpha = 90^0$), these vortices were not significant. The K-type vortex street started appearing at $\alpha < 80^0$ and became very clearly visible $\alpha = 60^0$. In Fig. 3a, the flow pattern at 60^0 angle of attack, indicates that the vortices in the vortex street are relatively closer to each other than that of at other lower angle of attacks. When the angle of attack reaches 52^0 (see Fig. 3b), the flow pattern is more clearly visible. As the angle of attack reaches 45^0, the flow structure becomes very clear with vortices are evenly spaced. In addition to this, at 45^0, the vortex street is the most stable. It can also be seen in the Fig 3(c) that the size of the vortices increases as they convected downstream. In terms of growing size with downstream distance, a similarity can be drawn with Karman vortex street in which the vortex size also increases as they travel downstream with the flow. At lower angle of attacks ($\alpha = 37^0$ & 30^0), the vortex street is still visible but becomes less stable than that of at $\alpha = 45^0$.

It should be noted that the evolution of this vortex street started at *Re* ~ 100 and its stability depends on the value of *Re*, as it can be clearly seen in Fig. 4. As stated above that these vortices are very stable at $\alpha = 45^0$, therefore keeping the $\alpha = 45^0$, *Re* was increased from 400 to 1000. It can be noted in Fig. 4 that at *Re* = 40^0 & 50^0, the vortex street is clearly visible. At *Re* = 400, apart from the size of the vortex which increases with downstream distance, its overall structure remain intact however at *Re* = 500, the shape of the vortex changes after a certain distance (~ 15 cm) downstream. At *Re* = 700, the vortices become unstable and decay, and almost disappear at *Re* > 1000. Strouhal number increases from 0.9 to 1.15 as the angle of attack is decreased from 60^0 to 30^0, and remains nearly constant to the change of Reynolds number.

In summary, three different states could be distinguished: the development of periodic vortex shedding (*Re* < 700), transition from periodic vortex shedding to chaotic motion (700 > *Re* > 1000), and a state in which the vortices disappear because of high water flow (*Re* > 1000). Despite these points, it must be stressed that the dye visualization images presented in Fig. 3 show the fully developed periodic wakes within the specified Reynolds numbers range. The images are considered to be indicative of the non-axisymmetric features that dominate the wake at the given Reynolds number range.

In addition, K-type vortex street is three-dimensional in nature (Fig. 5). It is evident from the top view (Fig. 3, and Fig. 4) that these vortices move both in X and in Y directions. Figure 5 shows a side view of the vortex street at *Re* = 700 and $\alpha = 45^0$ for the big plastic needle (Table 1). It can be clearly seen in the figure that these vortices not only move in X and Y-directions, but they also move in Z-direction making their overall movement three dimensional.

4. CONCLUSIONS

The flow past tall finite inclined cylinders' tip has been investigated using dye flow visualization technique at angle of attack 30^0 - 60^0 and *Re* in the range 100 - 2000. This flow poses challenges for experimental investigation and the aim of the present paper was to provide a complete flow picture. In the previous investigations, Park & Lee [47] and Pattenden *et al.* [48] presented the formation of the time-averaged tip vortices on the free end. However in those studies, the cylinders were mounted perpendicular to the tunnel floor and also perpendicular to the incoming flow. In this study, it was shown that the wake of the inclined cylinders' tip consisted of a counter rotating vortices. Despite counter rotating feature, the K-type vortices are significantly different from Karman vortices in terms of shape and their movement with the flow. The K-type vortices formed approximately at *Re* = 100 and convected with the flow in all three-dimensions substantially. The stability of these vortices depends on two parameters, a) angle of attack, and b) *Re*. It has been shown that the vortices become unstable above *Re* = 700 and almost disappear at *Re* > 1000.

5. REFERENCES

[1]. A. Roshko, On the development of turbulent wakes from vortex streets. Technical Report TN 1191, NACA, US Government Printing O4ce, Washington, DC. (1954a).

[2]. A. Roshko, On the drag and shedding frequency of two-dimensional blu1 bodies. Technical Report TN 3169, NACA, US Government Printing O4ce, Washington, DC, A (1954b)

[3]. C.H.K. Williamson, Oblique and parallel modes of vortex shedding in the wake of a circular cylinder at low Reynolds numbers. *Journal of Fluid Mechanics*, **206**, 579–627, (1989).

[4]. D. Birch, T. Lee, Investigation of the near-field tip vortex behind an oscillating wing. *Journal of Fluid Mechanics*, **544**, 201–241, (2005).

[5]. V.L. Okulov, On the stability of multiple helical vortices. *Journal of Fluid Mechanics*, **521**, 319-342, (2004).

[6]. V.L. Okulov, J.N. Sorensen, Stability of helical tip vortices in a rotor far wake. *Journal of Fluid Mechanics*, **576**, 1-25, (2007).

[7]. J.N. Sorensen, Aerodynamic aspects of wind energy conversion. *Annual Review of Fluid Mechanics*, **43**, 427-448, (2011).

[8]. J. Counihan, Adiabatic atmospheric boundary layers: A review and analysis of data from the period 1880-1972. *Atmospheric Environment* **9**, 871–905, (1975).

[9]. N.J. Cook, Wind-tunnel simulation of adiabatic atmospheric boundary layer by roughness, barrier and mixing device method. *Journal of Wind Engineering and Industrial Aerodynamics*, **3**, 157–176, (1978).

[10]. K. Varshney, K. Poddar, Experiments on integral length scale control in atmospheric boundary layer wind tunnel. *Theoretical and Applied Climatology*, **106(1-2)**, 127–137, (2011).

[11]. K.Varshney, K. Poddar, Prediction of wind properties in urban environments using artificial neural network. *Theoretical and Applied Climatology*, **107(3-4)**, 579–590, (2012).

[12]. K. Varshney, Tailoring wind properties by various passive roughness elements in a boundary-layer wind tunnel. *International Journal of the Physical Sciences*, **7**(8), 1182-1186, (2012).

[13]. D.A. Wang, H.T. Pham, C.W. Chao, J.M. Chen, A piezoelectric energy harvester based on pressure fluctuations in K´arm´an vortex street. World Renewable Energy Congress, 8-13 May 2011, Link¨oping, Sweden, (2011).

[14]. C.H.K. Williamson, Vortex dynamics in the cylinder wake. *Annual Review of Fluid Mechanics*, **28**, 477–539, (1996).

[15]. M.M. Zdravkovich, Flow around Circular Cylinders. Fundamentals, Oxford Scientific Publisher **Vol (1)**, (1997a].

[16]. M.M. Zdravkovich, Flow around Circular Cylinders. Fundamentals, Oxford Scientific Publisher **Vol (2)**, (1997b].

[17]. E. Marumo, K. Suzuki, T. Sato, A turbulent boundary layer disturbed by a cylinder. *Journal of Fluid Mechanics*, **87**, 121–141, (1997).

[18]. P.W. Bearman, M.M. Zdravkovich, Flow around a circular cylinder near a plane boundary. *Journal of Fluid Mechanics*, **89**, 33–47, (2005).

[19]. T. Karasudani, M. Funakoshi, Evolution of a vortex street in the far wake of a circular cylinder. *Fluid Dynamics Research*, **14(6)**, 331–352, (1994).

[20]. J. Wu, J. Sheridan, M.C. Welsh, K. Hourigan, Three-dimensional vortex structures in a cylinder wake. *Journal of Fluid Mechanics*, **312**, 201–222, (1996).

[21]. B.S. Carmo, S.J. Sherwin, P.W. Bearman, R.H.J. Willden, Wake transition in the flow around two circular cylinders in staggered arrangements. *Journal of Fluid Mechanics*, **597**, 1–29, (2008).

[22]. A.C. Mandal, J. Dey, An experimental study of boundary layer transition induced by a cylinder wake. *Journal of Fluid Mechanics*, **684**, 60–84, (2011).

[23]. A. Nicolle, I. Eames, Numerical study of flow through and around a circular array of cylinders. *Journal of Fluid Mechanics*, **679**, 1–31, (2011).

[24]. B.R. Noack, On the flow around a circular cylinder. Part I: laminar and transitional regime. Z Angew Math Mech, **79**, 223–226, (1999a).

[25]. B.R. Noack, On the flow around a circular cylinder. Part II: turbulent regime. Z Angew Math Mech, **79**, 227–230, (1999b).

[26]. A. Okajima, Strouhal numbers of rectangular cylinders. *Journal of Fluid Mechanics*, **123**, 379–398, (1982).

[27]. C. Norberg, Flow around rectangular cylinders: pressure forces and wake frequencies. *Journal of Wind Engineering and Industrial Aerodynamics*, **47**, 187–196, (1993).

[28]. J.H. Choi, S.J.Lee, Flow characteristics around an inclined elliptic cylinder in a turbulent boundary layer. *Journal of Fluids and Structure*, **15**, 1123–1135, (2011).

[29]. W.J. Devenport, M.C. Rife, S.I. Liapis, G.J. Follin, The structure and development of a wing-tip vortex. *Journal of Fluid Mechanics*, **312**, 67–106, (1996).
[30]. G.K. Batchelor, Axial flow in trailing line vortices. *Journal of Fluid Mechanics,* **20**, 645–658, (1964).
[31]. S.I. Green, A.J. Acosta, Unsteady flow in trailing vortices. *Journal of Fluid Mechanics,* **227**, 107–134, (1991).
[32]. P.R. Spalart, Airplane trailing vortices. *Annual Review of Fluid Mechanics*, **30**, 107–138, (1998).
[33]. T. Gerz, F. Holzapfel, Wing-tip vortices, turbulence, and the distribution of emissions. *AIAA*, **37**, 1270–1276, (1999).
[34]. G.J. Sheard, M.J. Fitzgerald, K. Ryan, Cylinders with square cross-section: wake instabilities with incidence angle variation. *Journal of Fluid Mechanics*, **630**, 43–69, (2009).
[35]. D.H. Yoon, K.S. Yang, C.B. Choi, Flow past a square cylinder with an angle of incidence. *Physics of Fluids*, **22**, 043603-(1-12), (2010).
[36]. A. Sohanka, C. Norberg, L. Davidson, Low Reynolds number flow around a square cylinder at incidence: study of blockage, onset of vortex shedding and outlet boundary condition. *International Journal of Numerical Methods in Fluids*, **26**: 39–56, (1998).
[37]. A. Sohanka, C. Norberg, L. Davidson, Simulation of three-dimensional flow around a square cylinder at moderate Reynolds numbers. *Physics of Fluids*, **11(2)**, 288–306, (1999).
[38]. K. Varshney, P.K. Panigrahi, Artificial neural network control of a heat exchanger in a closed flow air circuit. *Applied Soft Computing*, **5**, 441–465, (2005).
[39]. A. Cramer, K. Varshney, T. Gundrum, G. Gerbeth, Experimental study on the sensitivity and accuracy of electric potential local flow measurements. *Flow Measurement and Instrumentation*, **17**, 1–11, (2006).
[40]. K. Varshney, I. Shapiro, Y. Bronsnick, J. Holahan, Air bypass in vertical stack water source heat pumps. *HVAC&R Research*, **17(5),** 692–709, (2011).
[41]. K. Varshney, J. E. Rosa, and I. Shapiro, Method to diagnose window failures and measure U-factors on site. *International Journal of Green Energy***, 9**(3), 280-296, (2012).
[42]. K. Varshney, S. Chang, Z.J. Wang, The kinematics of falling maple seeds and the initial transition to a helical motion. *Nonlinearity*, **25**(1), C1–C8, (2012).
[43]. A. Roulund, B.M. Sumer, J. Fredsoe, J. Michelsen, Numerical and experimental investigation of flow and scour around a circular pile. *Journal of Fluid Mechanics*, **534**, 351–401, (2005).
[44]. B.M. Sumer, N. Christiansen, J. Fredsoe, The horseshoe vortex and vortex shedding around a vertical wall-mounted cylinder exposed to waves. *Journal of Fluid Mechanics*, **332**, 41–70, (1997).
[45]. M.J. Shelley, J. Zhang, Flapping and bending bodies interacting with fluid flows. *Annual Review of Fluid Mechanics*, **43**, 449–465, (2011).
[46]. H.A. Khaledi, H.I. Andersson, On vortex shedding from a hexagonal cylinder. *Physics Letters A*, **5**, 4007–4021, (2011).
[47]. G.S. West, C.J. Apelt, The effects of tunnel blockage and aspect ratio on the mean flow past a circular cylinder with Reynolds numbers between 104 and 105. *Journal of Fluid Mechanics*, **114**, 361–377, (1982).
[48]. C.W. Park, S.J Lee, Flow structure around a finite circular cylinder embedded in various atmospheric boundary layers. *Fluid Dynamics Research*, **30**, 197–215, (2002).
[49]. R.J. Pattenden, S.R. Turnock, X. Zhang, Measurements of the flow over a low-aspect ratio cylinder mounted on a ground plane. *Experiments in Fluids*, **39**, 10–21, (2005).
[50]. G. Palau-Salvador, T. Stoesser, J. Frohlich, M. Kappler, W.Rodi, Large eddy simulations and experiments of flow around finite-height cylinders. *Flow Turbulence and Combustion*, **84**, 239–275, (2008).
[51]. R. Hain, C.J. Kahler, D. Michaelis, Tomographic and time resolved PIV measurements on a finite cylinder mounted on a flat plate. *Experiments in Fluids*, **45**: 715–724, (2008).